Communications in Theoretical Physics

Commun. Theor. Phys. **77** (2025) 115801 (7pp) https://doi.org/10.1088/1572-9494/add43e
CSTR: 32041.14.CTPadd43e

Oscillation quenching of coupled limit-cycle oscillators with shear diversity

Hua-Jian Yu[1], **Zhi-Gang Zheng**[2,*] **and Can Xu**[2,*]

[1] School of Mathematical Sciences, Huaqiao University, Quanzhou 362021, China
[2] Institute of Systems Science and College of Information Science and Engineering, Huaqiao University, Xiamen 361021, China

E-mail: zgzheng@hqu.edu.cn and xucan@hqu.edu.cn

Received 3 February 2025, revised 25 March 2025
Accepted for publication 6 May 2025
Published 4 July 2025

Abstract

Coupled oscillator systems often exhibit collective dynamics as a consequence of their mutual heterogeneous interactions. Recent studies have highlighted the importance of shear diversity, an inhomogeneous pattern, in influencing the collective behavior of complex systems. Here, we investigate the quenching dynamics occurring within a network of limit-cycle oscillators that are globally coupled by taking into account both the shear diversity and the heterogeneous natural frequencies that are assumed to be statistically independent. Beyond the phase-only model considered in previous studies, we propose a general approach for identifying the critical criteria, demonstrating the instability of the incoherent state, by retaining the responses of both amplitudes and phases. This study advances the understanding of the role of heterogeneous couplings in interacting dynamical agents, offering valuable insights into the quenching phenomena observed in complex systems.

Keywords: limit-cycle oscillators, shear diversity, oscillation quenching

(Some figures may appear in colour only in the online journal)

1. Introduction

Networks of nonlinear coupled oscillators offer a powerful framework for understanding and capturing diverse emergent phenomena across various fields of science and technology. This research field has generated growing interest in the theoretical challenges arising at the interface of statistical mechanics and nonlinear dynamics [1–3].

The main challenge in current research lies in analyzing coupled systems with a high number of independent parameters, which have been shown to exhibit a wide range of intriguing collective phenomena and structural patterns. Theoretical studies have primarily concentrated on phase-only models, often neglecting amplitude effects under the assumption of weak coupling [4, 5].

Among coupled phase oscillators, one of the most prominent collective behaviors is the onset of synchronization. Specifically, synchronization describes a collective behavior where phase oscillators progressively align their motion through dissipative interactions, ultimately reaching a state of unison over time [6–10].

However, when the system involves interacting oscillators with strong coupling, amplitude effects become important, extending beyond the phase-only models. In this regard, amplitude variations cannot be ignored, leading to a variety of intriguing cooperative phenomena, as reported in many studies [11–22].

One particularly notable dynamic feature is oscillation quenching, a self-organized collective phenomenon that arises from the stabilization of an unstable equilibrium state [23]. In particular, this phenomenon is crucial for understanding and controlling associated oscillatory dynamics across various physical, chemical, biological and engineered systems [11, 24].

Previous studies of oscillation quenching have typically focused on systems where there is no correlation between the natural frequencies and oscillators' amplitudes. However, recent investigations have shown that the presence of such a correlation, encoded by the shear diversity (nonisochronicity), can significantly shape the quenching dynamics of the oscillator systems [25–32]. For example, [30–32] suggested that

* Authors to whom any correspondence should be addressed.

shear diversity can significantly modify the critical point for synchronization onset within the phase reduction framework (weak coupling limit). However, to the best of our knowledge, no systematic study has been conducted to investigate the effects of shear diversity on oscillation quenching when both amplitude and phase responses are considered simultaneously.

In this study, we examine the quenching dynamics within a globally coupled oscillator network, considering both phase and amplitude responses. Specifically, we demonstrate that shear diversity has a critical influence on determining the onset of quenching dynamics. Beyond the phase-only model, we present a detailed stability analysis in terms of the limit-cycle kinetic theory with a continuous limit, which enables us to analytically locate the critical threshold characterizing the disappearance of oscillation quenching. Notably, we show that the interaction between the heterogeneous natural frequencies and shear diversity has a decisive impact on determining the characteristic equations and the eigenspectrum structure of the linearized system. Thus, our study offers valuable insights into the emergent mechanism of oscillation quenching in systems with inherent shear diversity, which can inform the design and control of oscillatory dynamics in complex systems.

The analytical framework is systematically developed as follows. In section 2, we formulate the nonlinear dynamical system of coupled limit-cycle oscillators incorporating shear diversity. Section 3 includes a linear stability analysis of the incoherent state within the thermodynamic limit ($N \to \infty$), establishing the critical point through spectral decomposition of the continuum operator. In section 4, we investigate the effect of shear diversity on the critical coupling for various distributions. Finally, section 5 concludes the study.

2. Dynamical model with shear diversity

We begin by considering a dynamical model characterized by a system of limit-cycle oscillators with global coupling and disorder, which is

$$\dot{z}_j = [1 + \mathrm{i}(\omega_j + q_j) - (1 + \mathrm{i}q_j)\,|z_j|^2]z_j + \frac{K}{N}\sum_{k=1}^{N}(z_k - z_j). \tag{1}$$

Here, $j = 1, 2, \ldots, N$ represents the index of oscillators. The complex variable $z_j(t) = x_j(t) + \mathrm{i}y_j(t)$ is the state of the jth oscillator at time t, with the overdot indicating the time derivative. ω_j denotes the natural frequency of the jth oscillator. $N \gg 1$ represents the system size and $K > 0$ characterizes the overall coupling strength between oscillators.

Remarkably, q_j accounts for the shear (or non-isochronicity), quantifying the dependence of the frequency and amplitude of the jth oscillator introduced in [30]. Typically, the natural frequencies and shears of equation (1) are distributed according to the densities $g(\omega)$ and $h(q)$, respectively. Here and in the following, we assume that $\{\omega_j\}$ and $\{q_j\}$ are independent random variables, i.e. the joint probability density of ω and q can be expressed as $p(\omega, q) = g(\omega)h(q)$. Furthermore, we assume that $g(\omega)$ and $h(q)$ are unimodal and symmetric distributions; namely, $g(\omega)$ and $h(q)$ are even functions and are non-increasing in the intervals $\omega > 0$, $q > 0$, respectively.

The vast majority of works concerning equation (1) made the assumption that the heterogeneity solely originates from the intrinsic frequencies, i.e. $q_j \equiv 0$. However, as reported in [30–32], the shear diversity, serving as a form of external fluctuation, must be considered to capture the underlying inhomogeneity of the oscillatory medium.

The coupling strategy presented in equation (1) extends the Stuart–Landau model, which provides the canonical description of interacting systems in the vicinity of the supercritical transition to oscillatory behavior. When there is no coupling ($K = 0$), the oscillators evolve independently, exhibiting limit-cycle motion with a unit radius following their respective natural frequencies and shears, i.e., $z_j(t) \sim \mathrm{e}^{\mathrm{i}(\omega_j + q_j)t}$. Upon introducing coupling, the cessation of oscillation occurs, resulting in the system reaching a stable state at equilibrium positions.

In [30–32], the authors attempted to explore the impact of shear diversity on oscillator quenching dynamics. In particular, they identified that shear diversity profoundly shapes the critical point for the emergence of collective synchronization. However, all previous investigations were limited to models based solely on phase dynamics, neglecting the impact of amplitude on the oscillators, and assumed weak coupling. In this work, we aim to advance and improve the stability analysis by retaining both the phase and amplitude responses, thereby offering a comprehensive approach for identifying the critical conditions that lead to the instability of the incoherent state in the presence of shear diversity.

3. Linear stability analysis

In this section, we focus on the stability of the incoherent state, where each oscillator moves independently along a circular trajectory determined by its natural frequency and shear, with varying radii. As highlighted previously, the incoherent state refers to a special form of quenching dynamics that essentially differs from other quenching states, such as amplitude death and oscillation death [33]. The stability of the incoherent state is characterized at the macroscopic scale, rather than being evident in the individual dynamics of the oscillators. Put differently, the incoherent state is defined by a zero macroscopic variable (mean-field), whereas the microscopic dynamics can exhibit rapid temporal fluctuations. To investigate the impact of shear diversity on the threshold for incoherent state instability, we undertake a comprehensive linear stability analysis that extends beyond the phase reduction framework outlined in [30–32].

To continue, it is useful to define an order parameter expressed as follows

$$Z(t) = R(t)\mathrm{e}^{\mathrm{i}\Theta(t)} = \frac{1}{N}\sum_{k=1}^{N} z_k(t), \tag{2}$$

where the complex quantity $Z(t)$ represents the center of mass of the configuration $\{z_k\}$ on the two-dimensional complex space, with $R(t)$ and $\Theta(t)$ corresponding to its modulus and phase angle, respectively. Thus, the evolution equation in equation (1) can be reformulated into a mean-field approximation, which leads to

$$\dot{z_j} = [1 - K + \mathrm{i}(\omega_j + q_j) - (1 + \mathrm{i}q_j)\,|z_j|^2]z_j + KZ. \quad (3)$$

In the polar coordinates, $z_j(t) = r_j(t)\mathrm{e}^{\mathrm{i}\theta_j(t)}$, the mean-field equation in equation (3) can be rewritten as two corresponding sets of differential equations

$$\dot{r_j} = (1 - K - r_j^2)r_j + K\,\mathrm{Re}(Z\mathrm{e}^{-\mathrm{i}\theta_j}), \quad (4)$$

$$\dot{\theta_j} = \omega_j + q_j - q_j r_j^2 + \frac{K}{r_j}\mathrm{Im}(Z\mathrm{e}^{-\mathrm{i}\theta_j}). \quad (5)$$

To perform the stability analysis of the incoherent state, we now express differential equations (4) and (5) in the limit of large N. Alternatively, equation (1) can be represented by a distribution function $\rho(r, \theta, \omega, q, t)$, in such a way that $\rho\mathrm{d}r\mathrm{d}\theta\mathrm{d}\omega\mathrm{d}q$ corresponds to the proportion of oscillators within the ranges $(r, r + \mathrm{d}r) \cup (\theta, \theta + \mathrm{d}\theta) \cup (\omega, \omega + \mathrm{d}\omega) \cup (q, q + \mathrm{d}q)$ at the specified time t. Additionally, the distribution function must comply with the normalization condition

$$\int_0^\infty \mathrm{d}r \int_0^{2\pi} \mathrm{d}\theta \int_{-\infty}^{\infty} \mathrm{d}\omega \int_{-\infty}^{\infty} \mathrm{d}q\rho(r, \theta, \omega, q, t) \times g(\omega)h(q) = 1. \quad (6)$$

Similarly, in the continuous limit, the order parameter is given by

$$Z(t) = \int_0^\infty \mathrm{d}r \int_0^{2\pi} \mathrm{d}\theta \int_{-\infty}^{\infty} \mathrm{d}\omega \int_{-\infty}^{\infty} \mathrm{d}q \times r\mathrm{e}^{\mathrm{i}\theta}\rho(r, \theta, \omega, q, t)g(\omega)h(q). \quad (7)$$

For simplicity, we have dropped the index of each oscillator in the continuous limit.

As for the incoherent state, all the oscillators move at their respective natural frequencies and shears on the circle $r_j = \sqrt{1 - K}$, i.e. the introduction of the coupling between the oscillators reduces the amplitude of the individual limit cycles from 1 to $\sqrt{1 - K}$. As a result, the distribution of the incoherent state is expressed as

$$\rho_0(r, \theta, \omega, q) = \frac{\delta(r - \sqrt{1 - K})}{2\pi}, \quad (8)$$

in which $\delta(\cdot)$ indicates the Dirac delta function. Rather than equation (1), the probability distribution satisfies the continuity equation of the form

$$\frac{\partial \rho}{\partial t} + \boldsymbol{\nabla} \cdot (\rho \boldsymbol{v}) = 0, \quad (9)$$

where $\boldsymbol{\nabla}$ represents the vector field divergence and the flow field is given by $\boldsymbol{v} = (\dot{r}, r\dot{\theta})$. Consequently, the continuity equation in terms of polar representation leads to

$$\frac{\partial \rho}{\partial t} + \frac{\partial}{\partial r}(\rho\dot{r}) + \frac{\partial}{\partial \theta}(\rho\dot{\theta}) = 0, \quad (10)$$

with

$$\dot{r} = (1 - K - r^2)r + \frac{K}{2}(Z\mathrm{e}^{-\mathrm{i}\theta} + \bar{Z}\mathrm{e}^{\mathrm{i}\theta}), \quad (11)$$

and

$$\dot{\theta} = \omega + q - qr^2 + \frac{K}{r}\frac{1}{2\mathrm{i}}(Z\mathrm{e}^{-\mathrm{i}\theta} - \bar{Z}\mathrm{e}^{\mathrm{i}\theta}). \quad (12)$$

From this point onward, "¯" will denote the complex conjugate. It should be emphasized that the vector field divergence is expressed in polar form $\left(\boldsymbol{\nabla} = \frac{\partial}{\partial r} + \frac{1}{r}\frac{\partial}{\partial \theta}\right)$.

Next, we perform a linearization of equation (10) around the fixed point given in equation (8). To achieve this, we apply a small perturbation to equation (8), that is

$$\rho(r, \theta, \omega, q, t) = \frac{\delta(r - \sqrt{1 - K})}{2\pi} + \delta\rho(r, \theta, \omega, q, t). \quad (13)$$

Owing to the normalization condition, the perturbated function satisfies

$$\int_0^\infty \mathrm{d}r \int_0^{2\pi} \mathrm{d}\theta \int_{-\infty}^{\infty} \mathrm{d}\omega \int_{-\infty}^{\infty} \mathrm{d}q\delta\rho(r, \theta, \omega, q, t) = 0. \quad (14)$$

As a result, the corresponding order parameter under the perturbation takes the form of

$$\delta Z(t) = \int_0^\infty \mathrm{d}r \int_0^{2\pi} \mathrm{d}\theta \int_{-\infty}^{\infty} \mathrm{d}\omega \int_{-\infty}^{\infty} \mathrm{d}q \times r\mathrm{e}^{\mathrm{i}\theta}\delta\rho(r, \theta, \omega, q, t)g(\omega)h(q). \quad (15)$$

Given that the distribution is 2π-periodic in θ, it follows that its Fourier series can be expressed as

$$\delta\rho(r, \theta, \omega, q, t) = \sum_{n=-\infty}^{\infty} \delta\rho_n(r, \omega, q, t)\mathrm{e}^{\mathrm{i}n\theta}, \quad (16)$$

in which $\delta\rho_n(r, \omega, q, t)$ represents the nth Fourier coefficient. It is worth noting that $\delta\rho_0 = 0$ as a result of the normalization condition in equation (14) and that $\delta\rho_n = \delta\bar{\rho}_{-n}$ due to the real-valued nature of $\delta\rho$. As can be observed from equation (15), the order parameter is exclusively determined by $\delta\rho_{-1}$, implying that higher-order Fourier coefficients do not contribute to the subsequent analysis. Thus, it is adequate to focus on the first Fourier subspace for further analysis.

In accordance with the linear stability analysis approach, we assume the forms $\delta\rho_{\pm 1}(t) = \delta\rho_{\pm 1}\mathrm{e}^{\lambda t}$ and $\delta Z(t) = \delta Z\mathrm{e}^{\lambda t}$. By substituting these expressions into equation (10) and matching the coefficients of the terms $\mathrm{e}^{\pm\mathrm{i}\theta}$, we derive the linear evolution equation for the first-order Fourier mode, which is given by

$$[\lambda - \mathrm{i}(\omega + q - qr^2)]\delta\rho_{-1} + \frac{\partial}{\partial r}[(1 - K - r^2)r\delta\rho_{-1}] = \frac{K\delta Z}{4\pi}\left[\frac{\delta(r - \sqrt{1 - K})}{r} - \delta'(r - \sqrt{1 - K})\right], \quad (17)$$

where $\delta'(\cdot)$ represents the differential of the Dirac delta function with respect to its argument. Notably, the specific structure of the right-hand term of equation (17) allows us to adopt the following assumption for $\delta\rho_{-1}$, which leads to

$$\delta\rho_{-1} = \frac{K\delta Z}{4\pi}[C_1(\omega, q)\delta(r - \sqrt{1-K}) + C_2(\omega, q)\delta'(r - \sqrt{1-K})], \tag{18}$$

where $C_{1,2}(\omega, q)$ are the constants that need to be determined.

By inserting equation (18) to equation (17) and applying the properties for the Dirac delta function, i.e.

$$f(x)\delta(x-a) = f(a)\delta(x-a) \tag{19}$$

and

$$f(x)\delta'(x-a) = f(a)\delta'(x-a) - f'(a)\delta(x-a). \tag{20}$$

This leads to a closed-form equation for the coefficients $C_{1,2}$, given by

$$[\lambda - \mathrm{i}(\omega + qK)]C_1 - 2\sqrt{1-K}q\mathrm{i}C_2 = \frac{1}{\sqrt{1-K}} \tag{21}$$

and

$$[\lambda - \mathrm{i}(\omega + qK)]C_2 + 2(1-K)C_2 = -1. \tag{22}$$

Straightforward computations yield

$$C_1 = \frac{1}{\sqrt{1-K}[\lambda - \mathrm{i}(\omega + qK)]} - \frac{2\sqrt{1-K}q\mathrm{i}}{[\lambda + 2(1-K) - \mathrm{i}(\omega + qK)][\lambda - \mathrm{i}(\omega + qK)]} \tag{23}$$

and

$$C_2 = -\frac{1}{\lambda + 2(1-K) - \mathrm{i}(\omega + qK)}. \tag{24}$$

By combining equation (18) and equation (23)∼equation (24) with equation (15), we derive the order parameter under the perturbation, resulting in

$$\begin{aligned}\delta Z &= \int_0^\infty \mathrm{d}r \int_0^{2\pi} \mathrm{d}\theta \int_{-\infty}^\infty g(\omega)\mathrm{d}\omega \int_{-\infty}^\infty h(q)\mathrm{d}q r\mathrm{e}^{\mathrm{i}\theta}\delta\rho_{-1}\mathrm{e}^{-\mathrm{i}\theta} \\ &= 2\pi\int_0^\infty \mathrm{d}r \int_{-\infty}^\infty g(\omega)\mathrm{d}\omega \int_{-\infty}^\infty h(q)\mathrm{d}q r\delta\rho_{-1} \\ &= \frac{K\delta Z}{2}\int_0^\infty \mathrm{d}r \int_{-\infty}^\infty g(\omega)\mathrm{d}\omega \int_{-\infty}^\infty h(q)\mathrm{d}q \\ &\quad \times r[C_1\delta(r - \sqrt{1-K}) + C_2\delta'(r - \sqrt{1-K})] \\ &= \frac{K\delta Z}{2}\int_{-\infty}^\infty g(\omega)\mathrm{d}\omega \int_{-\infty}^\infty h(q)\mathrm{d}q \\ &\quad \times \left[\frac{1}{\lambda - \mathrm{i}(\omega + qK)} + \frac{1}{\lambda + 2(1-K) - \mathrm{i}(\omega + qK)} \right. \\ &\quad \left. - \frac{2(1-K)q\mathrm{i}}{[\lambda + 2(1-K) - \mathrm{i}(\omega + qK)][\lambda - \mathrm{i}(\omega + qK)]}\right].\end{aligned} \tag{25}$$

Ultimately, we obtain the self-consistent equation that governs the eigenvalues of the linearized system around the incoherent state, which gives

$$\frac{2}{K} = I_1 + I_2 - I_3, \tag{26}$$

with

$$I_1 = \int_{-\infty}^\infty \int_{-\infty}^\infty \frac{1}{\lambda - \mathrm{i}(\omega + qK)} g(\omega)h(q)\mathrm{d}\omega\mathrm{d}q, \tag{27}$$

$$I_2 = \int_{-\infty}^\infty \int_{-\infty}^\infty \frac{1}{\lambda + 2(1-K) - \mathrm{i}(\omega + qK)} g(\omega)h(q)\mathrm{d}\omega\mathrm{d}q, \tag{28}$$

$$I_3 = \int_{-\infty}^\infty \int_{-\infty}^\infty \frac{2(1-K)q\mathrm{i}}{\lambda + 2(1-K) - \mathrm{i}(\omega + qK)} \times \frac{1}{\lambda - \mathrm{i}(\omega + qK)} g(\omega)h(q)\mathrm{d}\omega\mathrm{d}q. \tag{29}$$

It is evident that the stability of the incoherent state is entirely determined by the real parts of the eigenvalues λ. In particular, the linear stability condition mandates that all eigenvalues lie in the left half of the complex plane.

The incoherent state becomes linearly unstable when the eigenvalues move across the imaginary axis. In particular, due to the symmetrical properties of $g(\omega)$ and $h(q)$, λ is shown to be real. The critical point K_c, indicating the onset of instability in the incoherent state, is located by applying the critical condition $\lambda \to 0^+$. This is because, in the case of continuous parameter variation, the stability of the system is generally determined by the sign of the eigenvalues, whereas oscillation quenching is typically triggered when λ crosses a critical value. Here, instability occurs when λ changes from negative to positive; therefore, the first instability point must correspond to $\lambda \to 0^+$, which is

$$\frac{1}{K_c} = \frac{\pi}{2}\int_{-\infty}^\infty g(-qK_c)h(q)\mathrm{d}q + \int_{-\infty}^\infty \int_{-\infty}^\infty \frac{1-K_c}{\omega + qK_c} \times \frac{\omega + q(2+K_c)}{(\omega + qK_c)^2 + 4(1-K_c)^2} g(\omega)h(q)\mathrm{d}\omega\mathrm{d}q. \tag{30}$$

Considering the special forms $g(\omega)$ and $h(q)$, the critical coupling strength K_c may be evaluated analytically. For instance, if $h(q) = \delta(q)$ (vanishing shear diversity), we have that

$$\frac{1}{K_c} = \frac{\pi}{2}g(0) + \int_{-\infty}^\infty \frac{1-K_c}{\omega^2 + 4(1-K_c)^2} g(\omega)\mathrm{d}\omega. \tag{31}$$

The implicit dependence of K_c on frequency distribution (intrinsic diversity) recovers the results of the classical Stuart–Landau model [14].

4. Mathematical consequences of shear diversity

In order to appreciate the impacts of shear diversity on the critical threshold, we next showcase several scenarios by specifying on some distributions of $g(\omega)$ and $h(q)$.

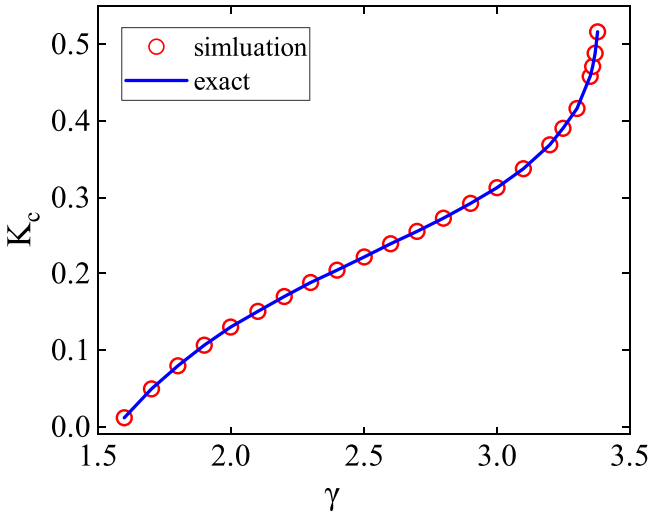

Figure 1. The critical coupling strength K_c as a function of the uniform distribution parameter γ is shown. The blue solid line corresponds the theoretical prediction by equation (34), while the red circles represent the results of numerical simulations with $N = 50000$.

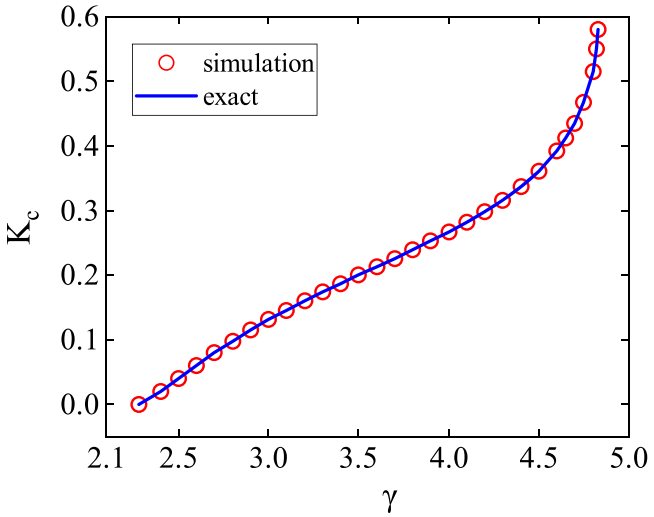

Figure 2. The critical coupling strength K_c as a function of the parabolic distribution parameter γ is shown. The blue solid line corresponds the theoretical prediction by equation (36), while the red circles represent the results of numerical simulations with $N = 50000$.

We begin by examining the scenario of identical oscillators, i.e. $g(\omega) = \delta(\omega)$. In this scenario, the closed form deciding the critical coupling strength K_c is expressed as

$$\frac{1}{K_c} = \frac{\pi h(0)}{2K_c} + \frac{(1-K_c)(2+K_c)}{K_c} \times \int_{-\infty}^{\infty} \frac{1}{(qK_c)^2 + 4(1-K_c)^2} h(q)\mathrm{d}q. \tag{32}$$

To proceed, we exemplify three typical distributions of shear to elucidate the critical coupling. For the scenario involving a uniform distribution, i.e.

$$h(q) = \begin{cases} \dfrac{1}{2\gamma}, & q \in (-\gamma, \gamma) \\ 0, & \text{otherwise;} \end{cases} \tag{33}$$

here, γ is interpreted as a measure describing the shear diversity. Therefore, the critical coupling strength is given by the following transcendental equation, which yields

$$\frac{1}{K_c} = \frac{\pi}{4K_c\gamma} + \frac{(1-K_c)(2+K_c)}{K_c} \frac{\arctan\left(\frac{K_c\gamma}{2-2K_c}\right)}{2K_c\gamma - 2K_c^2\gamma}. \tag{34}$$

Correspondingly, equation (34) should be solved numerically to obtain the relation between K_c and γ (figure 1).

For the scenario of a parabolic distribution, i.e.

$$h(q) = \begin{cases} \frac{3}{4}\frac{\gamma^2 - q^2}{\gamma^3}, & q \in (-\gamma, \gamma) \\ 0, & \text{otherwise} \end{cases} \tag{35}$$

and γ reflects the shear diversity. Consequently, the coupling strength K_c is determined by the following complicated transcendental equation, which reads

$$\frac{1}{K_c} = \frac{3\pi}{8K_c\gamma} + \frac{(1-K_c)(2+K_c)}{K_c}\left[-\frac{3((K_c-1)\pi + K_c\gamma)}{2K_c^3\gamma^3} - \frac{3(K_c-1)\arctan\left(\frac{2K_c-2}{K_c\gamma}\right)}{K_c^3\gamma^3} + \frac{3\arctan\left(\frac{K_c\gamma}{2-2K_c}\right)}{4K_c\gamma - 4K_c^2\gamma}\right]. \tag{36}$$

Also, the general relation between K_c and γ is illustrated in figure 2.

We now turn to consider the case in which the shear distribution has an infinite support. Specifically, $h(q)$ is selected as a Lorentzian distribution expressed as

$$h(q) = \frac{\gamma/\pi}{q^2 + \gamma^2}, \; q \in (-\infty, \infty). \tag{37}$$

Notably, the critical coupling strength K_c can be represented by a straightforward expression, resulting in

$$K_c = \frac{1-\gamma}{1 - 3\gamma + \gamma^2}. \tag{38}$$

The associated results are depicted in figure 3.

In contrast to case of the identical oscillators, we next consider the nonidentical scenario with distributed frequencies to further examine the influences of both types of diversity on the critical threshold. To this end, we choose $g(\omega)$ and $h(q)$ to be the Lorentzian form with different widths, i.e.

$$g(\omega) = \frac{\delta/\pi}{\omega^2 + \delta^2}, \; h(q) = \frac{\gamma/\pi}{q^2 + \gamma^2}, \; \omega, q \in (-\infty, \infty). \tag{39}$$

Unlike the situations of the identical oscillators discussed above, we point out that it is difficult to obtain an explicit formula of the closed form concerning the critical coupling. Nevertheless, the results can be solved numerically by

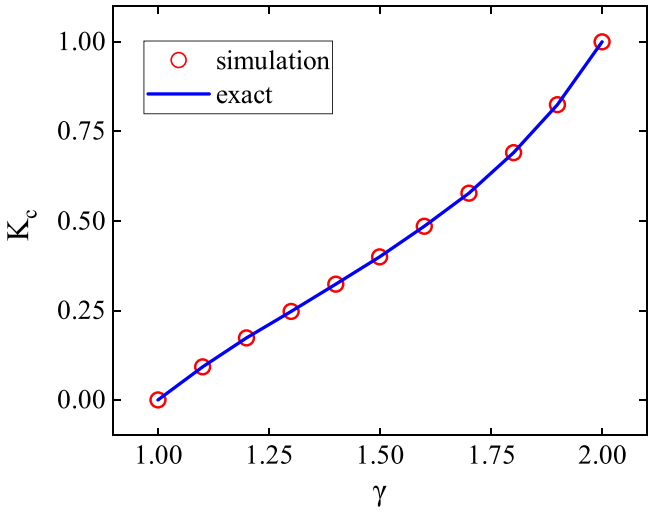

Figure 3. The critical coupling strength K_c as a function of the Lorentzian distribution parameter γ is shown. The blue solid line corresponds the theoretical prediction by equation (38), while the red circles represent the results of numerical simulations with $N = 50000$.

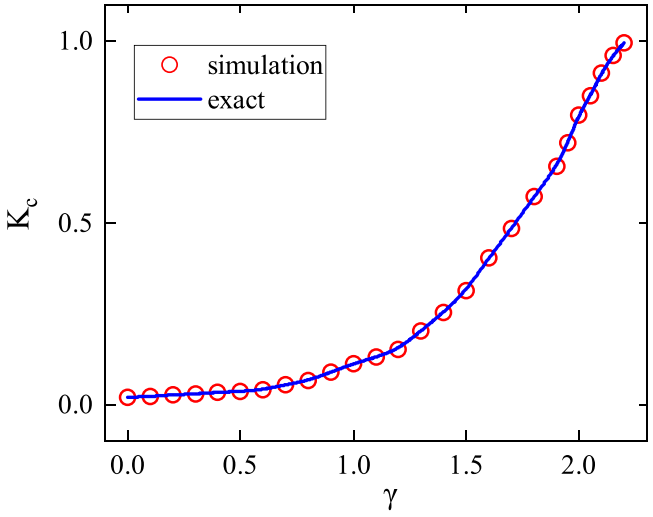

Figure 4. The critical coupling strength K_c as a function of the Lorentzian distribution parameters γ and $\delta = 0.01$ is shown. The blue solid line corresponds the theoretical prediction through numerical integration equation (30), while the red circles represent the results of numerical simulations with $N = 50000$.

inserting equation (39) into equation (30) as shown in figure 4.

Taken together, the critical coupling strength K_c as functions of shear diversity parameters are illustrated in figures 1–4. It is shown that the critical coupling strength K_c exhibits monotonically increasing behaviors with the diversity parameters for both identical and nonidentical oscillator populations, and the analytical predictions (lines) coincide well with the numerical simulations (circles). These plots demonstrate that the increment of shear diversity tend to inhibit the instability of the incoherent state, thereby making it more difficult for the system to reach the coherent states.

Previous research has demonstrated that shear diversity plays a crucial role in shaping the onset of synchronization within the context of phase reduction models. Interestingly, it was found that increasing shear diversity delays the critical threshold for phase synchronization onset, with this threshold diverging at a specific value of the shear diversity parameter. When both the amplitude and phase effects are considered simultaneously, we remark that the tendency of stabilizing the incoherent state inducing by the shear diversity is maintained. In other words, the shear diversity is prone to postpone the occurrence of the rhythmic states. However, in contrast to the phase-only models, we highlight that the critical coupling strength K_c in the amplitude-phase scenario remains finite. This is due to the fact that the interplay between the phases and amplitudes of the oscillators demands that the existent condition for the incoherent state is $K \in [0, 1]$. Nevertheless, we emphasize that the critical coupling exists only in a certain range of γ (shear diversity) for the identical oscillators, whereas it exists in the whole range of γ for the nonidentical oscillator populations given that $K_c < 1$. Mathematically, the particular dependence of the critical coupling K_c on the shear diversity parameter γ is governed by the transcendental properties of the characteristic equations. Beyond the existent region of K_c, the system gives rise to fascinating rhythmic dynamics that will be reported elsewhere.

5. Conclusion

In summary, we explored the quenching dynamics induced by the shear diversity in a globally coupled oscillator system by taking into account both phase and amplitude responses. As reported in previous studies, the distributed shear in the phase-only models (e.g. Kuramoto-like models) hinders the emergence of phase synchronization and even makes it impossible at a certain range of the shear diversity [30]. In this work, we demonstrated that the amplitude and phase responses combine together to affect the onset of collective dynamics under the influence of shear diversity. Specifically, we found that the added shear diversity tends to inhibit the occurrence of coherent behavior, even when amplitude effects are suppressed. Nevertheless, we revealed that the critical coupling K_c, featuring the instability of the incoherent state (macroscopic quenching dynamics), exhibits a monotonically increasing function with respect to the parameter of shear diversity that can never diverge owing to the restricted region of the incoherent state.

Theoretically, we developed a general framework for systemically performing linear stability analysis of incoherent states that goes beyond phase-reduction models. We analytically derived the eigenvalue spectrum of the linearized system, explicitly accounting for the nonlinear amplitude-phase coupling inherent in limit-cycle ensembles. Consequently, the critical coupling strengths were formulated in terms of several transcendental equations (equations (34) and (36)). This study establishes a robust theoretical framework that advances the investigation of diversity-mediated amplitude suppression phenomena in nonlinear dynamic systems, while simultaneously developing a unified analytical paradigm for characterizing synchronization stability in networks of coupled limit-cycle oscillators.

Acknowledgments

This work is supported by the National Natural Science Foundation of China (Grants No.12375031 and No.11905068), and the Natural Science Foundation of Fujian Province, China (Grant No. 2023J01113).

ORCID iDs

Hua-Jian Yu https://orcid.org/0009-0009-5412-4432

References

[1] Stankovski T, Pereira T, McClintock P V E and Stefanovska A 2017 Coupling functions: universal insights into dynamical interaction mechanisms *Rev. Mod. Phys.* **89** 045001
[2] Ghosh D, Frasca M, Rizzo A, Majhi S, Rakshit S, Alfaro-Bittner K and Boccaletti S 2022 The synchronized dynamics of time-varying networks *Phys. Rep.* **949** 1–63
[3] Zheng Z, Xu C, Fan J, Liu M and Chen X 2024 Order parameter dynamics in complex systems: from models to data *Chaos* **34** 022101
[4] Winfree A T 1967 Biological rhythms and the behavior of populations of coupled oscillators *J. Theor. Biol.* **16** 15–42
[5] Kuramoto Y 1984 *Chemical Oscillations Waves, and Turbulence* (Berlin: Springer)
[6] Strogatz S H 2000 From Kuramoto to Crawford: exploring the onset of synchronization in populations of coupled oscillators *Physica* D **143** 1–20
[7] Acebrón J A, Bonilla L L, Pérez Vicente C J, Ritort F and Spigler R 2005 The Kuramoto model: a simple paradigm for synchronization phenomena *Rev. Mod. Phys.* **77** 137–85
[8] Pikovsky A and Rosenblum M 2015 Dynamics of globally coupled oscillators: progress and perspectives *Chaos* **25** 097616
[9] Xu C, Wang X and Skardal P S 2022 Generic criterion for explosive synchronization in heterogeneous phase oscillator populations *Phys. Rev. Res.* **4** L032033
[10] Yu H, Zheng Z and Xu C 2023 Deterministic correlations enhance synchronization in oscillator populations with heterogeneous coupling *Phys. Rev.* E **108** 054203
[11] Zou W, Senthilkumar D V, Zhan M and Kurths J 2021 Quenching, aging, and reviving in coupled dynamical networks *Phys. Rep.* **931** 1–72
[12] Mirollo R E and Strogatz S H 1990 Amplitude death in an array of limit-cycle oscillators *J. Stat. Phys.* **60** 245–62
[13] Aronson D G, Ermentrout G B and Koppel N 1990 Amplitude response of coupled oscillators *Physica* D **41** 403–49
[14] Matthews P C, Mirollo R E and Strogatz S H 1991 Dynamics of a large system of coupled nonlinear oscillators *Physica* D **52** 293–331
[15] Reddy D V R, Sen A and Johnston G L 1998 Time delay induced death in coupled limit cycle oscillators *Phys. Rev. Lett.* **80** 5109
[16] Atay F M 2003 Distributed delays facilitate amplitude death of coupled oscillators *Phys. Rev. Lett.* **91** 094101
[17] Daido H and Nakanishi K 2004 Aging transition and universal scaling in oscillator networks *Phys. Rev. Lett.* **93** 104101
[18] Karnatak R, Ramaswamy R and Prasad A 2007 Amplitude death in the absence of time delays in identical coupled oscillators *Phys. Rev.* E **76** 035201(R)
[19] Banerjee T and Ghosh D 2014 Transition from amplitude to oscillation death under mean-field diffusive coupling *Phys. Rev.* E **89** 052912
[20] Bi H, Hu X, Zhang X, Zou Y, Liu Z and Guan S 2014 Explosive oscillation death in coupled Stuart–Landau oscillators *Europhys. Lett.* **108** 50003
[21] Zhao N, Sun Z, Yang X and Xu W 2018 Explosive death of conjugate coupled Van der Pol oscillators on networks *Phys. Rev.* E **97** 062203
[22] Dutta S, Verma U K and Jalan S 2023 Solitary death in coupled limit cycle oscillators with higher-order interactions *Phys. Rev.* E **108** L062201
[23] Koseska A, Volkov E and Kurths J 2013 Transition from amplitude to oscillation death via turing bifurcation *Phys. Rev. Lett.* **111** 024103
[24] Zou W, Senthilkumar D V, Nagao R, Kiss I Z, Tang Y, Koseska A, Duan J and Kurths J 2015 Restoration of rhythmicity in diffusively coupled dynamical networks *Nat. Commun.* **6** 7709
[25] Hakim V and Rappel W J 1992 Dynamics of the globally coupled complex Ginzburg–Landau equation *Phys. Rev.* A **46** R7347
[26] Cross M C and Hohenberg P C 1993 Pattern formation outside of equilibrium *Rev. Mod. Phys.* **65** 851
[27] Daido H and Nakanishi K 2006 Diffusion-induced inhomogeneity in globally coupled oscillators: Swing-by mechanism *Phys. Rev. Lett.* **96** 054101
[28] Blasius B, Montbrió E and Kurths J 2003 Anomalous phase synchronization in populations of nonidentical oscillators *Phys. Rev.* E **67** 035204
[29] Montbrió E and Blasius B 2003 Using nonisochronicity to control synchronization in ensembles of nonidentical oscillators *Chaos* **13** 291–308
[30] Montbrió E and Pazó D 2011 Shear diversity prevents collective synchronization *Phys. Rev. Lett.* **106** 254101
[31] Pazó D and Montbrió E 2011 The Kuramoto model with distributed shear *Europhys. Lett.* **95** 60007
[32] Montbrió E and Pazó D 2011 Collective synchronization in the presence of reactive coupling and shear diversity *Phys. Rev.* E **84** 046206
[33] Xu C and Yu H 2024 Stability of oscillation quenching in coupled oscillator populations with heterogeneous coupling *Phys. Rev.* E **110** 064221